

Effect of Peripheral Layer on Peristaltic Transport of a Micropolar Fluid

K. M. Prasad, G. Radhakrishnamacharya

Department of Mathematics and Humanities
National Institute of Technology
Warangal-506004, India
grk.nitw@yahoo.com

Received: 2008-03-13 **Revised:** 2008-11-20 **Published online:** 2009-03-10

Abstract. Peristaltic transport of two fluid model with micropolar fluid in the core region and Newtonian fluid in the peripheral layer is studied under the assumptions of long wavelength and low Reynolds number. The linearised equations governing the flow are solved and closed form expressions for pressure rise, time averaged flux and frictional force have been obtained. The effects of various parameters on these flow variables have been studied. It is found that the pressure rise increases with micropolar parameter (m) and central mean radius (η), but decreases with coupling number (N) and viscosity ratio ($\bar{\mu}$). The frictional force (\bar{F}) decreases with coupling number (N) and viscosity ratio ($\bar{\mu}$) but increases with micropolar parameter (m) and mean radius of central layer (η).

Keywords: peristaltic transport, peripheral layer, micropolar fluid, core region radius, amplitude ratio, frictional force.

1 Introduction

Peristaltic transport is a form of fluid transport that occurs when progressive wave of area contraction or expansion propagates along the length of a distensible tube containing the liquid. It appears to be the major mechanism for urine transport in ureter, food mixing and chyme movement in intestines, transport of spermatozoa in cervical canal, transport of bile in bile ducts and so on. Roller and finger pumps use peristalsis to pump corrosive materials so as to prevent direct contact of the fluid with the pump's internal surfaces.

The study of peristalsis has received considerable attention in last three decades mainly because of its importance in biological systems and industrial applications. Several investigators have analyzed the peristaltic motion of both Newtonian and non-Newtonian fluids in mechanical as well as physiological systems (Fung and Yih [1], Burns and Parkes [2], Shapiro et al. [3], Selverov and Stone [4], Xiao and Damodaran [5], Misra and Rao [6], Radhakrishnamacharya and Srinivasulu [7], Maruthi Prasad and Radhakrishnamacharya [8], Muthu et al. [9]).

The effect of peripheral layer on peristaltic flow has received some attention in the recent past in the view of its relevance in physiological systems. Hence, Shukla et al. [10] studied the effect of peripheral layer on peristaltic transport of a bio-fluid. Srivastava and Srivastava [11] investigated the effect of peristalsis on a flow of a two-layered model with Casson fluid in the core region and Newtonian fluid in the peripheral layer. Ramachandra Rao and Usha [12] investigated the peristaltic transport of two immiscible fluids in a circular tube under the assumptions of long-wavelength and low Reynolds number. Misra and Pandey [13] considered a two-dimensional channel flow of a power-law fluid surrounded by a peripheral layer of power-law fluid having viscosity different from that of core fluid.

It is realized that the model of micropolar fluid introduced by Eringen [14] serves as an appropriate model for blood (Arıman and Turk [15]). These fluids consist of rigid, randomly oriented (or spherical) particles suspended in a viscous medium where the deformation of particles is ignored. Basically, these fluids can support couple stresses and body couples and exhibit micro rotational and micro inertial effects. It can be observed that micropolar fluid model takes care of the rotation of fluid particles by means of an independent kinematic vector called micro rotation vector. Therefore, the model of a micropolar fluid may be more appropriate for any bio-fluids. Hence, Muthu et al. [16] and Srinivasacharya et al. [17] studied peristaltic transport of a micropolar fluid. The steady stagnation flow towards a permeable vertical surface immersed in micropolar fluid is investigated by Anuar Ishak et al. [18]. The peristaltic motion of micropolar fluid in a circular cylindrical tube with elastic wall properties has been studied by Muthu et al. [19]. Hayat and Ali [20] investigated the effects of an endoscope on peristaltic flow of micropolar fluid.

However, peristaltic motion of a two-layer model with micropolar fluid has not received much attention. It is known that the viscosity of the fluid in the peripheral region is different from that in the core region in many vessels in physiological systems like vasomotion of some blood vessels, motion in ductus efferentes of the male reproductive tract, transport of spermatozoa in the cervical canal, transportation of chyme in the oesophagus (Misra and Pandey [13]). This study may help in understanding the interaction of micropolar fluid and peripheral layer in peristaltic transport with particular reference to the above mentioned systems.

Keeping the above in view, we considered the effect of peristalsis on flow of two-layered model with micropolar fluid in the core region and Newtonian fluid in the peripheral layer. Assuming that the wavelength of the peristaltic wave is large in comparison to the mean radius of the tube, the linearised equations of motion have been solved and closed form expressions for pressure rise and time averaged flux have been obtained. The effects of various parameters on these flow variables have been studied.

2 Mathematical formulation

Consider the peristaltic transport of a micropolar fluid surrounded coaxially by Newtonian fluid in an axisymmetric tube of radius a , with core radius a_1 . Choosing the cylindrical polar coordinate system (R, θ, Z) the wall deformation due to propagation of an infinite

train of peristaltic waves is given by

$$R = H(Z, t) = a + b \sin \frac{2\pi}{\lambda}(Z - ct), \quad (1)$$

where b is the amplitude, λ is the wave length and c is the speed of the wave.

Following Shukla et al. [10], the nature of the interface is same as that of wall movement as shown in Fig. 1.

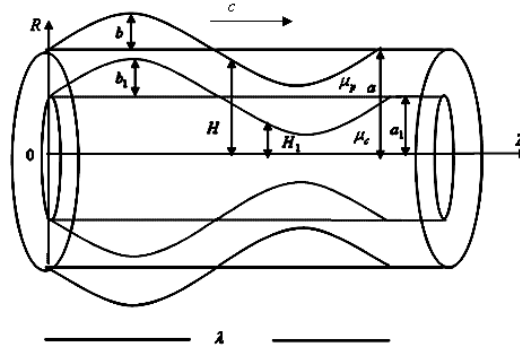


Fig. 1. Peristaltic transport in a tube.

Hence the geometry of the central layer is given by

$$H_1(Z, t) = a_1 + b_1 \sin \frac{2\pi}{\lambda}(Z - ct). \quad (2)$$

Using the transformation

$$r = R, \quad \theta = \theta, \quad z = Z - ct, \quad w_z = W_z - c, \quad w_r = W_r$$

from a stationary to a moving frame of reference, the equations of motion in two regions are given as follows:

(a) Peripheral region ($H_1(z) \leq r \leq H(z)$):

$$\frac{\partial p}{\partial z} = \mu_p \nabla^2 w_1, \quad (3)$$

$$\frac{\partial p}{\partial r} = 0, \quad (4)$$

where $\nabla^2 = (\frac{\partial^2}{\partial r^2} + \frac{1}{r} \frac{\partial}{\partial r} + \frac{\partial^2}{\partial z^2})$, w_1 is the component of velocity in z direction, p is the pressure and μ_p is the viscosity of Newtonian fluid in peripheral region.

(b) Core region ($0 \leq r \leq H_1(z)$).

The constitutive equations and equations of motion for micropolar fluid flow are given by

(Srinivasacharya et al. [17])

$$\nabla \cdot \bar{w} = 0, \quad (5)$$

$$\rho(\bar{w} \cdot \nabla \bar{w}) = -\nabla p + k(\nabla \times \bar{w}) + (\mu_c + k)\nabla^2 \bar{w}, \quad (6)$$

$$\rho j(\bar{w} \cdot \nabla \bar{g}) = -2k\bar{g} + k(\nabla \times \bar{w}) - \gamma(\nabla \times \nabla \times \bar{g}) + (\alpha + \beta + \gamma)\nabla(\nabla \cdot \bar{g}), \quad (7)$$

where \bar{w} is the velocity vector, \bar{g} is the microrotation vector, p is the fluid pressure, ρ and j are the fluid density and microgyration parameters, μ_c is viscosity of micropolar fluid in core region. k, α, β and γ are the material constants and satisfy the following inequalities (Eringen [15]):

$$2\mu_c + k \geq 0, \quad k \geq 0, \quad 3\alpha + \beta + \gamma \geq 0, \quad \gamma \geq |\beta|.$$

Since the flow is axisymmetric, all the variables are independent of θ as hence for this flow, the velocity vector is given by $\bar{w} = (w_r, 0, w_z)$ and microrotation vector is $\bar{g} = (0, v_\theta, 0)$.

Introducing the following non-dimensional quantities

$$\begin{aligned} h' &= \frac{H}{a}, \quad h'_1 = \frac{H_1}{a}, \quad r' = \frac{r}{a}, \quad z' = \frac{z}{\lambda}, \quad w'_1 = \frac{w_1}{c}, \quad p' = \frac{a^2 p}{\lambda \mu_c c}, \\ w'_r &= \frac{\lambda w_r}{ca}, \quad w'_z = \frac{w_z}{c}, \quad v'_\theta = \frac{v_\theta}{a^2}, \quad t' = \frac{ct}{\lambda}, \quad j' = \frac{j}{a^2} \end{aligned}$$

into equations (3) to (7) and dropping the primes, we get

$$\frac{\partial p}{\partial z} = \frac{1}{r} \frac{\partial}{\partial r} \left(\bar{\mu} r \frac{\partial}{\partial r} \right) w_1, \quad (8)$$

$$\frac{\partial p}{\partial r} = 0, \quad (9)$$

$$\frac{\partial w_r}{\partial r} + \frac{w_r}{r} + \frac{\partial w_z}{\partial z} = 0, \quad (10)$$

$$\begin{aligned} R_e \delta^3 \left(w_r \frac{\partial w_r}{\partial r} + w_z \frac{\partial w_r}{\partial z} \right) \\ = -\frac{\partial p}{\partial r} + \frac{\delta^2}{1-N} \left(-N \frac{\partial v_\theta}{\partial z} + \frac{\partial^2 w_r}{\partial r^2} + \frac{1}{r} \frac{\partial w_r}{\partial r} - \frac{w_r}{r^2} + \delta^2 \frac{\partial^2 w_r}{\partial z^2} \right), \end{aligned} \quad (11)$$

$$\begin{aligned} R_e \delta \left(w_r \frac{\partial w_z}{\partial r} + w_z \frac{\partial w_z}{\partial z} \right) \\ = -\frac{\partial p}{\partial z} + \frac{1}{N-1} \left(\frac{N}{r} \frac{\partial}{\partial r} (r v_\theta) + \frac{\partial^2 w_z}{\partial r^2} + \frac{1}{r} \frac{\partial w_z}{\partial r} + \delta^2 \frac{\partial^2 w_z}{\partial z^2} \right), \end{aligned} \quad (12)$$

$$\begin{aligned} \frac{j R_e \delta (1-N)}{N} \left(w_r \frac{\partial v_\theta}{\partial r} + w_z \frac{\partial v_\theta}{\partial z} \right) \\ = -2v_\theta + \left(\delta^2 \frac{\partial w_r}{\partial z} - \frac{\partial w_z}{\partial r} \right) + \frac{2-N}{m^2} \left[\frac{\partial p}{\partial r} \left(\frac{1}{r} \frac{\partial}{\partial r} (r v_\theta) \right) + \delta^2 \frac{\partial^2 v_\theta}{\partial z^2} \right], \end{aligned} \quad (13)$$

where $\bar{\mu} = \frac{\mu_p}{\mu_c}$ is the viscosity ratio, $\delta = \frac{a}{\lambda}$, $R_e = \frac{\rho a c}{\mu_c}$ is the Reynolds number, $N = \frac{k}{\mu_c + k}$ is the coupling number ($0 \leq N < 1$) and $m^2 = \frac{a^2 k (2\mu_c + k)}{\gamma (\mu_c + k)}$ is the micropolar parameter.

Using long wavelength approximation ($\delta \ll 1$) and neglecting inertial terms ($R_e = 0$), equations (11) to (13) reduce to

$$\frac{\partial p}{\partial r} = 0, \quad (14)$$

$$\frac{N}{r} \frac{\partial}{\partial r} (r v_\theta) + \left(\frac{\partial^2 w_z}{\partial r^2} + \frac{1}{r} \frac{\partial w_z}{\partial r} \right) = (1 - N) \frac{\partial p}{\partial z}, \quad (15)$$

$$2v_\theta + \frac{\partial w_z}{\partial r} + \frac{2 - N}{m^2} \frac{\partial}{\partial r} \left(\frac{1}{r} \frac{\partial}{\partial r} (r v_\theta) \right) = 0. \quad (16)$$

The non-dimensional boundary conditions are

$$w_1 = -1 \quad \text{at } r = h(z) = 1 + \varepsilon \sin[2\pi z], \quad (17)$$

$$\frac{\partial w_z}{\partial r} = 0 \quad \text{at } r = 0, \quad (18)$$

$$w_z \text{ is finite} \quad \text{at } r = 0, \quad (19)$$

$$v_\theta = 0 \quad \text{at } r = h_1(z) = \eta + \varepsilon_1 \sin[2\pi z], \quad (20)$$

$$w_1 = w_z \quad \text{at } r = h_1(z), \quad (21)$$

$$\bar{\mu} \frac{\partial w_1}{\partial r} = \frac{\partial w_z}{\partial r} - \frac{N}{1 - N} v_\theta \quad \text{at } r = h_1(z), \quad (22)$$

where ε ($\varepsilon = \frac{b}{a}$) is the amplitude ratio, $\eta = \frac{a_1}{a}$ and $\varepsilon_1 = \frac{b_1}{a}$.

3 Solution

Solving equation (8), subject to the boundary condition (17), we get

$$w_1 = \frac{1}{4\bar{\mu}} (r^2 - h^2) \frac{dp}{dz} + \frac{c_1}{\bar{\mu}} \log \left(\frac{r}{h} \right) - 1. \quad (23)$$

Equation (15) can be written as

$$\frac{\partial}{\partial r} \left(r \frac{\partial w_z}{\partial r} + N r v_\theta - (1 - N) \frac{r^2}{2} \frac{dp}{dz} \right) = 0. \quad (24)$$

Using equation (24) and (16), we get

$$\frac{\partial^2 v_\theta}{\partial r^2} + \frac{1}{r} \frac{\partial v_\theta}{\partial r} - \left(m^2 + \frac{1}{r^2} \right) v_\theta = \frac{m^2 (1 - N)}{2 - N} \frac{r}{2} \frac{dp}{dz} + \frac{m^2}{2 - N} \frac{c_2}{r}. \quad (25)$$

The general solution of equation (25) is

$$v_\theta = c_3(z) I_1(mr) + c_4(z) K_1(mr) - \frac{1 - N}{2 - N} \frac{r}{2} \frac{dp}{dz} + \frac{c_2}{N - 2} \frac{1}{r}, \quad (26)$$

where $I_1(mr)$ and $K_1(mr)$ are modified Bessel functions of first order and second order respectively.

Using equation (26) in (24) and solving for w_z , we get

$$w_z = c_2 \log r \frac{2}{2-N} + \frac{N}{m} [-c_3 I_0(mr) + c_4 K_0(mr)] + \frac{r^2}{4} \frac{dp}{dz} \frac{2(1-N)}{2-N} + c_5, \quad (27)$$

where I_0 and K_0 are modified Bessel functions of zeroth order.

Using the boundary conditions (18)–(22), the expressions for w_1 and w_z are given by

$$w_1 = \frac{1}{4\bar{\mu}} (r^2 - h^2) \frac{dp}{dz} + \frac{c_1}{\bar{\mu}} \log \left(\frac{r}{h} \right) - 1, \quad h_1(z) \leq r \leq h(z), \quad (28)$$

$$w_z = \frac{-N}{m} c_3 I_0(mr) + \left(\frac{1-N}{2-N} \right) \frac{dp}{dz} + c_5, \quad 0 \leq r \leq h_1(z), \quad (29)$$

where $c_1 = -N h_1(z) I_1(mh_1) \frac{2-N}{1-N} c_3$,

$$c_3 = \frac{\frac{1-N}{2-N} \frac{h_1}{2} \frac{dp}{dz}}{I_1(mh_1)},$$

$$c_5 = \left[\frac{h_1^2 - h^2}{4\bar{\mu}} - \left(\frac{1-N}{2-N} \right) \frac{h_1^2}{2} - N \frac{h_1^2}{2\bar{\mu}} \log \left(\frac{h_1}{h} \right) + \frac{N}{m} \left(\frac{1-N}{2-N} \right) \frac{h_1}{2} \frac{I_0(mh_1)}{I_1(mh_1)} \right] \frac{dp}{dz} - 1.$$

The dimensionless flux q ($q = \frac{q'}{\pi a^2 c}$) in the moving frame is given by

$$q = \int_0^{h_1} 2r w_z dr + \int_{h_1}^h 2r w_1 dr. \quad (30)$$

Substituting for w_1 and w_z from equation (28) and (29) in (30) and finally we get

$$q = 2c_3 \left(\frac{-N}{m^2} \right) I_1(mh_1) h_1 + \frac{1-N}{2-N} \frac{h_1^4}{4} \frac{dp}{dz} - \frac{(h^2 - h_1^2)^2}{8\bar{\mu}} \frac{dp}{dz} + h_1^2 c_5 + \frac{2c_1}{\bar{\mu}} \left[\frac{h_1^2}{4} - \frac{h^2}{4} - \frac{h_1^2}{2} \log \left(\frac{h_1}{h} \right) \right] - (h^2 - h_1^2). \quad (31)$$

From equation (31), we get

$$\frac{dp}{dz} = \frac{q + h^2}{S}, \quad (32)$$

where

$$S = - \frac{(h^2 - h_1^2)^2}{8\bar{\mu}} + \left(\frac{1-N}{2-N} \right) \frac{h_1^4}{4} + \frac{(h_1^2 - h^2) h_1^2}{4\bar{\mu}} - \left(\frac{1-N}{2-N} \right) \frac{h_1^4}{2} - \frac{N}{2\bar{\mu}} h_1^2 \log \left(\frac{h_1}{h} \right) + \frac{N}{m} \left(\frac{1-N}{2-N} \right) \frac{h_1^3}{2} \frac{I_0(mh_1)}{I_1(mh_1)} - \frac{N h_1^2}{m^2} \left(\frac{1-N}{2-N} \right) - \frac{N h_1^2}{\bar{\mu}} \left[\frac{h^2 - h_1^2}{4} - \frac{h_1^2}{2l} \log \left(\frac{h_1}{h} \right) \right].$$

The pressure drop over a wavelength Δp_λ is defined by

$$\Delta p_\lambda = - \int_0^1 \left(\frac{dp}{dz} \right) dz. \quad (33)$$

Substituting the expression $\frac{dp}{dz}$ in equation (33), we get

$$-\Delta p_\lambda = qL_1 + L_2, \quad (34)$$

where $L_1 = \int_0^1 \frac{dz}{S}$, $L_2 = \int_0^1 \frac{h^2}{S} dz$.

Following the analysis of Shapiro et al. [3], the time averaged flux over a period in the laboratory frame, \bar{Q} , is given by

$$\bar{Q} = 1 + \frac{\varepsilon^2}{2} + q. \quad (35)$$

Substituting equation (34) in (35), we get

$$\bar{Q} = 1 + \frac{\varepsilon^2}{2} - \left(\frac{\Delta p_\lambda}{L_1} + \frac{L_2}{L_1} \right). \quad (36)$$

The dimensionless frictional force F ($F = \frac{F'}{\pi\lambda c\mu}$) at the wall is given by

$$F = \int_0^1 h^2 \left(- \frac{dp}{dz} \right) dz. \quad (37)$$

4 Results

The effects of various parameters on pressure rise ($-\Delta p_\lambda$), pressure rise at zero time averaged flux ($\Delta p_{\lambda 0}$), time averaged flux at zero pressure rise (\bar{Q}_0) and frictional force (\bar{F}) have been computed using numerical integration by using mathematica 5.1 software and the results are graphically presented in Figs. 2–17.

It can be seen from Figs. 2–5 that the pressure rise ($-\Delta p_\lambda$) increases with the increase of the time averaged flux (\bar{Q}) for the fixed values of viscosity ratio ($\bar{\mu}$), mean radius of central radius (η), micropolar parameter (m) and amplitude ratio (ε). Further, it can be seen from Fig. 2 that the pressure rise ($-\Delta p_\lambda$) decreases with coupling number (N). It can be seen that the pressure rise decreases as viscosity ratio ($\bar{\mu}$) increases (Fig. 3). Also, Figs. 4 and 5 show that the pressure rise increases as the micropolar effect (m) increases and with mean radius of the central layer (η).

The pressure rise at zero time averaged flux ($\Delta p_{\lambda 0}$), an important flow variable, is calculated from the expression equation (33) by taking $\bar{Q}_0 = 0$ and the results are plotted in Figs. 6–9. It can be seen from Figs. 6 and 7 that ($\Delta p_{\lambda 0}$) decreases with the coupling number (N) and viscosity ratio ($\bar{\mu}$) but this decreases is significant only for values of

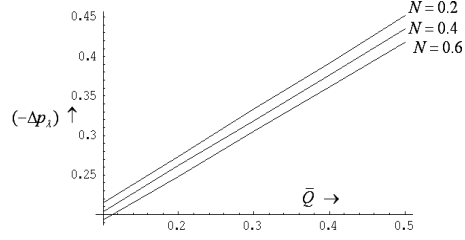


Fig. 2. Effect of \bar{Q} and N on $(-\Delta p_\lambda)$
($\bar{\mu} = 0.5, \eta = 0.5, \varepsilon = 0.4, m = 2$).

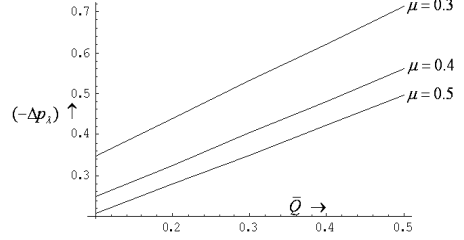


Fig. 3. Effect of \bar{Q} and $\bar{\mu}$ on $(-\Delta p_\lambda)$
($\eta = 0.5, \varepsilon = 0.4, N = 0.8, m = 2$).

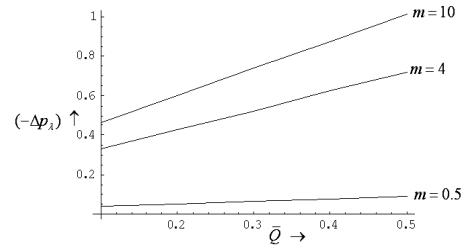


Fig. 4. Effect of \bar{Q} and m on $(-\Delta p_\lambda)$
($\eta = 0.5, \varepsilon = 0.4, N = 0.8, \bar{\mu} = 0.5$).

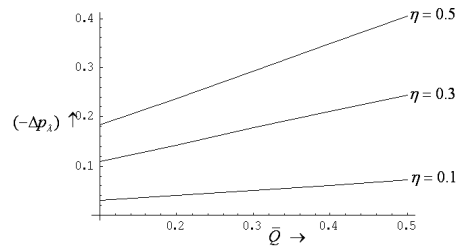


Fig. 5. Effect of \bar{Q} and η on $(-\Delta p_\lambda)$
($m = 2, \varepsilon = 0.4, N = 0.8, \bar{\mu} = 0.5$).

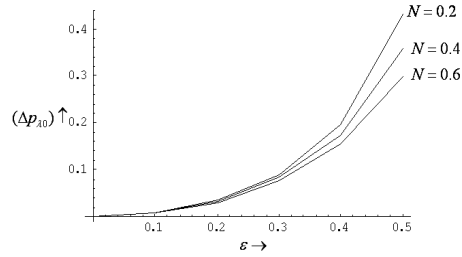


Fig. 6. Effect of ε and N on (Δp_{λ_0})
($m = 2, \eta = 0.8, \bar{\mu} = 0.5$).

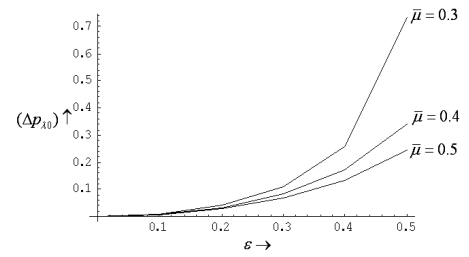


Fig. 7. Effect of ε and $\bar{\mu}$ on (Δp_{λ_0})
($m = 2, \eta = 0.8, N = 0.8$).

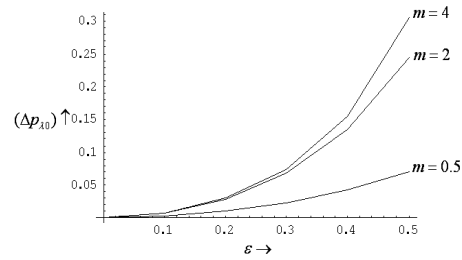


Fig. 8. Effect of ε and m on (Δp_{λ_0})
($\eta = 0.8, N = 0.8, \bar{\mu} = 0.5$).

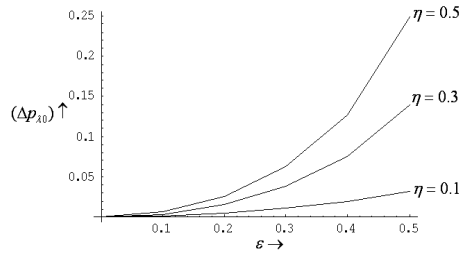


Fig. 9. Effect of ε and η on (Δp_{λ_0})
($m = 2, N = 0.8, \bar{\mu} = 0.5$).

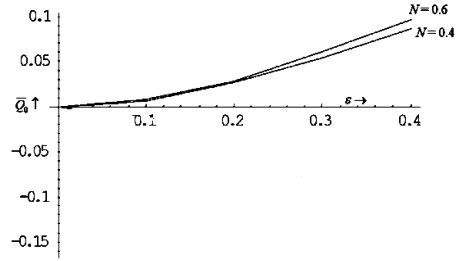


Fig. 10. Effect of ε and N on (\bar{Q}_0)
($m = 0.001, \eta = 0.8, \bar{\mu} = 0.5$).

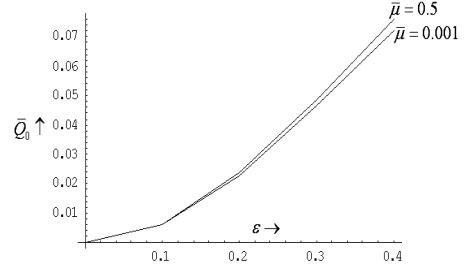


Fig. 11. Effect of ε and $\bar{\mu}$ on (\bar{Q}_0)
($m = 0.001, N = 0.8, \eta = 0.4$).

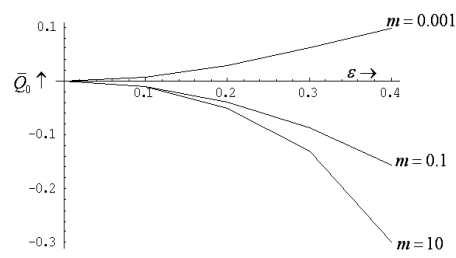


Fig. 12. Effect of ε and m on (\bar{Q}_0)
($N = 0.6, \eta = 0.4, \bar{\mu} = 0.5$).

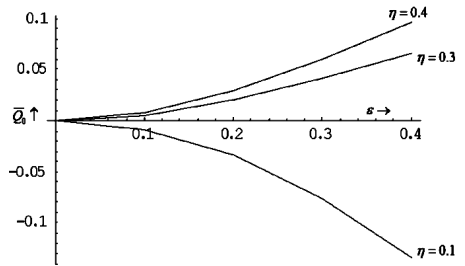


Fig. 13. Effect of ε and η on (\bar{Q}_0)
($m = 2, N = 0.8, \bar{\mu} = 0.5$).

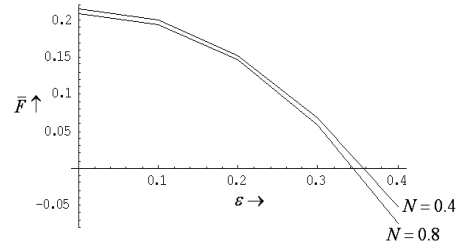


Fig. 14. Effect of ε and N on \bar{F} ($m = 10,$
 $\eta = 0.4, \bar{\mu} = 0.5, \Delta p_\lambda = 0.2$).

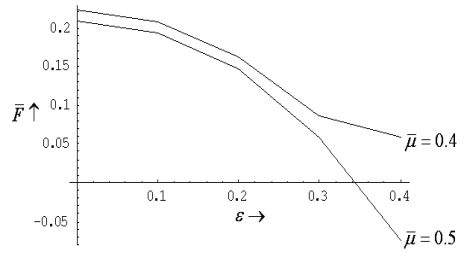


Fig. 15. Effect of ε and $\bar{\mu}$ on \bar{F} ($m = 10,$
 $N = 0.8, \eta = 0.4, \Delta p_\lambda = 0.2$).

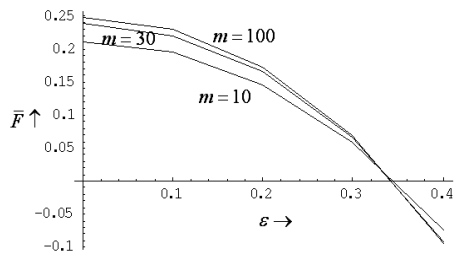


Fig. 16. Effect of ε and m on \bar{F} ($\bar{\mu} = 0.5,$
 $N = 0.8, \eta = 0.4, \Delta p_\lambda = 0.2$).

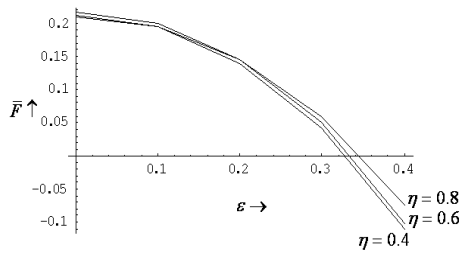


Fig. 17. Effect of ε and η on \bar{F} ($\bar{\mu} = 0.5,$
 $m = 10, N = 0.8, \Delta p_\lambda = 0.2$).

amplitude ratio (ε) beyond 0.3. However, $(\Delta p_{\lambda 0})$ increases with micropolar parameter (m) and mean radius of the central layer (η) (Figs. 8 and 9).

The effects of various parameters on time averaged flux at zero pressure rise (\bar{Q}_0), i.e., the time averaged flux \bar{Q} calculated for $\Delta p_{\lambda} = 0$, are shown in Figs. 10–13. It is observed that for fixed values other parameters, the time averaged flux at zero pressure rise increases with coupling number (N), viscosity ratio ($\bar{\mu}$) and mean radius of central layer (η), but this increase is insignificant for lower values of amplitude ratio ($\varepsilon \leq 0.2$). Further, \bar{Q}_0 decreases with micropolar parameter (m).

The variation of frictional force \bar{F} with various parameters is shown in Figs. 14 to 17. The frictional force decreases with the coupling number (N) and viscosity ratio ($\bar{\mu}$) (Figs. 14 and 15). However, Figs. 16 and 17 show that the frictional force increases with micropolar parameter (m) and mean radius of central layer (η).

The expressions for the flow variables reduce to those of Shapiro et al. [3] if we take the micropolar parameters to be zero and the peripheral layer to be absent.

5 Conclusion

Peristaltic flow of two-layered model with micropolar fluid in the core region and Newtonian fluid in the peripheral layer has been investigated under the long wavelength approximation. It is found that the pressure rise decreases with coupling number and viscosity ratio but increases with other micropolar parameter and mean radius of central layer. Also the frictional force decreases with coupling number and viscosity ratio but increases with mean radius of central layer and other micropolar parameter.

References

1. Y. C. Fung, C. S. Yih, Peristaltic transport, *Trans. ASME J. Appl. Mech.*, **35**, pp. 669–675, 1968.
2. J. C. Burns, T. Parkes, Peristaltic motion, *J. Fluid Mech.*, **29**, pp. 731–743, 1969.
3. A. H. Shapiro, M. Y. Jaffrin, S. L. Weinberg, Peristaltic pumping with long wavelengths at low Reynolds numbers, *J. Fluid Mech.*, **37**, pp. 799–825, 1969.
4. K. P. Selverov, H. A. Stone, Peristaltically driven channel flows with applications toward micromixing, *Phys. Fluids*, **13**, pp. 1837–1859, 2001.
5. Q. Xiao, M. Damodaran, A numerical investigation of peristaltic waves in circular tubes, *Int. J. Comput. Fluid Dyn.*, **16**, pp. 201–216, 2002.
6. M. Misra, A. R. Rao, Peristaltic transport of a Newtonian fluid in an asymmetric channel, *Z. Angew. Math. Phys.*, **54**, pp. 532–550, 2003.
7. G. Radhakrishnamacharya, Ch. Srinivasulu, Influence of wall properties on peristaltic transport with heat transfer, *C. R. Mechanique*, **335**, pp. 369–373, 2007.
8. K. Maruthi Prasad, G. Radhakrishnamacharya, Peristaltic transport of a Herschel-Bulkley fluid in a channel in the presence of magnetic field of low intensity, *Int. J. of Computational Intelligence and Applications*, **1**, pp. 71–81, 2007.

9. P. Muthu, B. V. Rathish Kumar, Peeyush Chandra, Peristaltic motion of micropolar fluid in circular cylindrical tubes: Effect of wall properties, *Appl. Math. Model.*, accepted, 2007.
10. J. B. Shukla, R. S. Parihar, B. R. P. Rao, S. P. Gupta, Effects of peripheral layer on peristaltic transport of a bio-fluid, *J. Fluid Mech.*, **97**, pp. 225–237, 1980.
11. L. M. Srivastava, V. P. Srivastava, Peristaltic transport of blood: Casson Model II, *J. Biomech.*, **17**, pp. 821–829, 1984.
12. A. Ramachandra Rao, S. Usha, Peristaltic transport of two immiscible viscous fluids in a circular tube, *J. Fluid Mech.*, **298**, pp. 271–28, 1995.
13. J. C. Misra, S. K. Pandey, Peristaltic transport of a non-Newtonian fluid with a peripheral layer, *Int. J. Eng. Sci.*, **37**, pp. 1841–1858, 1999.
14. A. C. Eringen, Theory of micropolar fluids, *J. Math. Mech.*, **16**, pp. 1–18, 1966.
15. T. Ariman, M. A. Turk, N. D. Sylvester, Applications of microcontinuum fluid mechanics, *Int. J. Eng. Sci.*, **12**, pp. 273–293, 1974.
16. P. Muthu, B. V. Rathish Kumar, Peeyush Chandra, On the influence of wall properties in the peristaltic motion of micropolar fluid, *ANZIAM J.*, **45**, pp. 245–260, 2003.
17. D. Srinivasacharya, M. Mishra, A. R. Rao, Peristaltic pumping of a micropolar fluid in a tube, *Acta Mech.*, **161**, pp. 165–178, 2003.
18. A. Ishak, R. Nazar, I. Pop, Stagnation flow of a micropolar fluid towards a vertical permeable surface, *Int. Commun. Heat Mass*, **35**, pp. 276–281, 2008.
19. P. Muthu, B. V. Rathish Kumar, P. Chandra, Peristaltic motion of micropolar fluid in circular cylindrical tubes: Effect of wall properties, *Appl. Math. Model.*, **32**(10), pp. 2019–2033, 2008.
20. H. Tasawar, A. Nasir, Effects of an endoscope on peristaltic flow of a micropolar fluid, *Math. Comput. Model.*, in press, 2007.